# Where the linearized Poisson–Boltzmann cell model fails: Spurious phase separation in charged colloidal suspensions

M. N. Tamashiro[a] and H. Schiessel
*Max-Planck-Institut für Polymerforschung, Ackermannweg 10, 55128 Mainz, Germany*

(Received 16 October 2002; accepted 11 April 2003)

The Poisson–Boltzmann (PB) spherical Wigner–Seitz cell model—introduced to theoretically describe suspensions of spherical charged colloidal particles—is investigated at the nonlinear and linearized levels. The linearization of the mean-field PB functional yields linearized Debye–Hückel-type equations agreeing asymptotically with the nonlinear PB results in the weak-coupling (high-temperature) limit. Both the canonical (fixed number of microions) as well as the semigrand-canonical (in contact with an infinite salt reservoir) cases are considered and discussed in a unified linearized framework. In disagreement with the exact nonlinear PB solution inside a Wigner–Seitz cell, the linearized theory predicts the occurrence of a thermodynamical instability with an associated phase separation of the homogeneous suspension into dilute (gas) and dense (liquid) phases, being thus a spurious result of the linearization. We show that these artifacts, although thermodynamically consistent with quadratic expansions of the nonlinear functional and osmotic pressure, may be traced back to the nonfulfillment of the underlying assumptions of the linearization. This raises questions about the reliability of the prediction of gas/liquid-like phase separation in deionized aqueous suspensions of charged colloids mediated by monovalent counterions obtained by linearized theories. © *2003 American Institute of Physics.*
[DOI: 10.1063/1.1579676]

## I. INTRODUCTION

The study of classical charged systems has received an increased renewed interest in view of many industrial applications:[1,2] Paint, petrochemicals, food, pharmaceuticals, cosmetics, diapers, sewage treatment, etc. Many environmental-friendly new materials are hydrosoluble due to the presence of ionizable groups that dissociate upon contact with water. In fact, their hydrosolubility is a result of the combination of Coulomb repulsion between fixed charged monomers and the mixing entropy maximized by the mobility in solution of the oppositely charged small counterions. Besides technological applications, charged macromolecules like lipid aggregates (bilayers, micelles, and vesicles), proteins and polynucleotides (including DNA and RNA) are also of fundamental importance in the biochemistry of living systems.[3,4] Furthermore, due to the availability of faster computers, many new insights in soft-matter physics come from Monte Carlo and molecular-dynamics simulations of charged systems.[5,6] These may be partially viewed as controlled theoretical experiments and provide a complementary approach to analytical treatments.

An ubiquitous case is that of mesoscopic charged colloidal particles (also called polyions or macroions) immersed in aqueous solution, which polarize the small mobile ions in their vicinity: Microions of opposite sign (counterions) are attracted to them, while like-sign microions (coions) are repelled. The theoretical description of these suspensions requires the understanding of the role of the electrostatic interactions between charged objects mediated by the surrounding aqueous ionic solution. In view of the many-body problem and the long-range nature of the Coulomb interaction, a statistical-mechanical treatment of the system is nontrivial. Within the primitive model[7] (PM) the molecular nature of the solvent is ignored (neglect of van der Waals and hydration forces) and the suspension is treated as a two-component system, comprised of the highly charged large polyions (and its neutralizing counterions) and oppositely charged pairs (anions and cations) of ionized salt particles. These are immersed in a continuous medium of dielectric constant $\epsilon$ and interact through the bare Coulomb potential with additional hard-sphere repulsion. In the PM it is implicitly assumed that the (hard) spheres have the same dielectric constant as the solvent, so there are no electrostatic image effects. For symmetric (in size and charge) electrolytes the PM reduces to the restricted primitive model (RPM) and a theoretical description for dilute solutions may be developed using the traditional Debye–Hückel (DH) theory for electrolytes,[8–10] with some improvements taking nonlinearities[11] into account or using integral-equation methods.[10,12] An extension of these theories for a colloidal suspension is nontrivial[12–14] in view of the huge asymmetry between poly- and microions. Compared to the symmetric case, nonlinearities are magnified and dominate in the strong asymmetric colloidal limit.

A mean-field approach to the PM, represented by the Poisson–Boltzmann (PB) approximation,[15–18] is often used in conjunction with the so-called Wigner–Seitz (WS) cell model. Both are discussed in Appendix A—this and all further Appendices will be presented in the form of an associated EPAPS document.[19] In view that even with these ap-

[a]Electronic mail: tamashir@mpip-mainz.mpg.de

 © 2003 American Institute of Physics

Downloaded 12 Jul 2004 to 194.95.63.241. Redistribution subject to AIP license or copyright, see http://jcp.aip.org/jcp/copyright.jsp

proximations the nonlinear PB equation can only be solved analytically in few particular cases, it would be very helpful to formulate a linearized version of the PB approximation for WS-cell models, in analogy to the DH approach to the RPM. We should remark, however, that the linearized version (at the mean-field level) of the WS-cell model does not include any *intercell* (neither polyion–microion nor microion–microion) correlations and *intracell* microion–microion correlations. This is in contrast to the traditional DH approach to the (symmetric) RPM, which automatically includes these correlations. While in the RPM the mean-field contribution vanishes,[20] in the PB WS-cell model it comes from the *intracell* polyion–microion correlations. Therefore, a more appropriate interpretation of the linearized equations to be obtained in the present work is that they correspond to an expansion about the weak-coupling or high-temperature limit of the mean-field equations.

Two decades after the first experimental evidences of attraction between like-charged spherical colloids mediated by monovalent counterions in bulk deionized aqueous suspensions, its existence is still under dispute. Under the mentioned conditions, electrostatic-stabilized colloidal crystals have been investigated by Ise *et al.*,[21] revealing the presence of empty regions (voids) inside the crystal. These experimental observations were interpreted as a coexistence between a dense crystalline phase and a dilute gas phase. Similar voids were also found experimentally in the fluid phase,[22] which, in analogy to the critical behavior of symmetric electrolytes, were interpreted as a coexistence between dilute (gas) and dense (liquid) fluid phases. Even fully equilibrated macroscopic gas–liquid phase separation has been reported,[23] although these experimental observations have been attributed to the presence of ionic impurities.[24]

From the theoretical point-of-view attractive interactions between like-charged spheres are observed only under special conditions. For example, they have been seen in Monte Carlo simulations in the presence of multivalent counterions[25–27] or when the low-temperature ordering of the discrete charges is taken into account.[28] Under the conditions described in the previous paragraph those controversial experimental findings are either attributed to the presence of long-range attractive electrostatic interactions between like-charged polyions,[29] by the presence of polyelectrolyte impurities,[30] or by state-independent volume terms[31,32] obtained by approximations that involve some kind of linearization: Random-phase approximation,[33–35] DH pair-distribution functions augmented by a variational approach for the polyion–polyion interactions,[36] linear-response approximation,[37] extended DH theory for asymmetric electrolytes,[38] mean-spherical approximation (MSA)[39] and symmetric PB and MSA.[40] Even though it has been argued by Overbeek and others[41] that the Sogami–Ise attraction[29] is due to inconsistencies in their thermodynamic treatment, the question does not seem to be settled yet and discussion is still in progress.[42] This attractive potential is in contrast to the generally accepted repulsive electrostatic component of the DLVO[43,44] (Derjaguin–Landau–Verwey–Overbeek) pair potential between like-charged polyions. However, the purely repulsive nature of the polyion–polyion effective pair potential does not preclude *a priori* the existence of a gas–liquid separation, as has been shown by Roij *et al.*[34] The focus on the polyion–polyion effective interactions overlooks the important contribution to the free energy due to the polyion–microion interactions.

Because most of the alternative analytical calculations to the Sogami–Ise attractive interaction potential requires some linearization procedure, the predicted gas–liquid coexistence should be analyzed with caution. In fact, no instabilities have been yet detected by Monte Carlo simulations in the presence of (explicit) *monovalent* counterions.[26,45] Further investigations with higher polyion valences should still be considered in order to confirm or invalidate these theoretical predictions. We should mention, however, that preliminary molecular-dynamics[46] as well as Monte Carlo[47] simulations in the presence of explicit *monovalent* counterions in the regime of high-surface charge and low density of polyions—where linearized theories predict phase separation—have shown no sign of any instabilities yet. Moreover, there are indications that the observed van der Waals-type loops are artifacts due to the linearization, these being drastically suppressed when nonlinearities are reintroduced in the theory by the use of renormalized charges.[48] Furthermore the linearization of the WS-cell semigrand-canonical PB functional—which describes (at the mean-field level) the system in electrochemical equilibrium with an infinite salt reservoir—yields negative-compressibility, thermodynamically unstable regions which are absent in a full nonlinear treatment.[49,50] Although many aspects of these artifacts for the semigrand-canonical case were already reported in the literature,[49] including a general analysis of the linearization scheme for various geometries, electrolyte compositions and arbitrary expansion densities,[50] we believe that there are still a few subtle points that need to be clarified, in particular concerning the relations between these spurious results and the thermodynamic self-consistency of alternative schemes of linearization.

The purpose of this paper is to perform a careful and detailed investigation about the linearization procedure in the well-controlled case of the PB WS-cell model. We believe this allows a broader audience—which might not be quite familiar with the more sophisticated treatments involving correlation-functions and integral-equations methods[33–40]—to understand the underlying physical assumptions of the approximate linearized theories. First we develop a linearization scheme suitable to the canonical (fixed amount of microions) case, by adopting an explicitly gauge-invariant approach. For the semigrand-canonical case, it has been argued by Deserno and von Grünberg[50] that the occurrence of unstable linearized equations of state depends on the way the linearization scheme is performed and on the osmotic-pressure definition. By extending our gauge-invariant approach to the semigrand-canonical ensemble, we try additionally to shed some light on this question. We show that thermodynamic stability and consistency are in fact independent concepts. The gauge-invariant forms of the equations of state allow to establish an explicit correspondence between their nonlinear and linearized versions. We will show, by using gauge-invariant forms for the electrostatic

Downloaded 12 Jul 2004 to 194.95.63.241. Redistribution subject to AIP license or copyright, see http://jcp.aip.org/jcp/copyright.jsp

potential, that there is a *unique* linearization (about the state-independent zeroth-order Donnan densities) that corresponds to the minimization of the associated linearized semigrand-canonical functional, which is also asymptotically exact (at the mean-field level) in the weak-coupling (high-temperature) limit. Therefore, the expansion of the nonlinear functional about the state-independent Donnan densities, originally proposed for the spherical geometry in the presence of symmetric electrolyte by von Grünberg *et al.*[49]—and generalized for arbitrary electrolyte compositions and geometries with analogous high symmetry in Ref. 50—is not only ''optimal,'' but it is asymptotically exact in the weak-coupling limit. The linearized equations, although thermodynamically self-consistent with quadratic expansions of the nonlinear ones, lead to artifacts when their underlying assumptions are not satisfied. In a related paper[51] explicit analytical comparison is performed for the planar case, where the exact nonlinear solution (at the mean-field level) can be obtained. We additionally show that the thermodynamical equivalence between the linearized canonical and semigrand-canonical formulations of the problem turns out to be nontrivial because of the Donnan effect (Appendix G), the ensemble invariance of the linearized equations only being possible with the inclusion of quadratic contributions in the linearized expansion densities.

The remainder of the paper is organized as follows: In Sec. II the salt-free model is introduced and the associated nonlinear equations are briefly presented. In Sec. III the linearization of the appropriate functional is performed, considering three distinct physical situations: The salt-free (in the presence of neutralizing counterions only) system introduced in Sec. II, with fixed amount of added monovalent salt (canonical ensemble) and in electrochemical equilibrium with an infinite monovalent salt reservoir (semigrand-canonical ensemble). Some concluding remarks are presented in Sec. IV. Several technical and subtle points are discussed in more detail in Appendices A–I, which are presented in the form of an associated EPAPS document.[19]

## II. NONLINEAR EQUATIONS

In this section we shortly summarize the framework in which the linearization procedure will be performed. For a detailed presentation and discussion—which emphasize the advantages of the use of a Lagrange multiplier leading to an explicitly gauge-invariant approach—we address the interested reader to Appendix A.

A suspension of polyions, whose hard cores occupy a volume fraction $\phi$, is treated within the WS-cell model, in which the physical properties of the system are studied by considering only one fixed polyion and its neutralizing counterions inside a WS cell. We will restrict ourselves to the case of spherical polyanions of radius $a$—each carrying a total charge $-Zq$ distributed uniformly on its surface, with $q$ being the elementary charge—inside a concentric spherical WS cell of radius $R=a/\phi^{1/3}$. The generalization to other highly symmetric geometries is straightforward, cf. Ref. 50.

We introduce the mean-field PB Helmholtz free-energy functional $\mathcal{F}[n_+(\boldsymbol{r})]$ associated to a single spherical WS cell

$$\beta\mathcal{F}[n_+(\boldsymbol{r})]=\frac{1}{8\pi\ell_B}\int \mathrm{d}^3\boldsymbol{r}\,[\nabla\psi(\boldsymbol{r})]^2 + \int \mathrm{d}^3\boldsymbol{r}\,n_+(\boldsymbol{r})\{\ln[n_+(\boldsymbol{r})\zeta_+^3]-1\}, \tag{1}$$

where $\beta^{-1}=k_BT$ is the thermal energy at temperature $T$, $\zeta_+$ is the thermal de Broglie wavelength of the counterions and $\ell_B=\beta q^2/\epsilon$ is the Bjerrum length with $\epsilon$ being the dielectric constant of the solvent. The integrations are performed over the free volume $V=(4\pi/3)(R^3-a^3)$ unoccupied by the polyion, $a\leqslant|\boldsymbol{r}|\leqslant R$. The total charge number density $\rho(\boldsymbol{r})$ is the sum of the continuous counterion density profile $n_+(\boldsymbol{r})$ and the negative surface charge on the polyion,

$$\rho(\boldsymbol{r})=n_+(\boldsymbol{r})-\frac{Z}{4\pi a^2}\delta^3(|\boldsymbol{r}|-a), \tag{2}$$

where $\delta^3$ is the three-dimensional Dirac delta function. The total charge number density is related to the reduced electrostatic potential $\psi(\boldsymbol{r})\equiv\beta q\Psi(\boldsymbol{r})$ by the (exact) Poisson equation, $\nabla^2\psi(\boldsymbol{r})=-4\pi\ell_B\rho(\boldsymbol{r})$. Functional minimization of $\mathcal{F}$ with respect to the counterion profile $n_+(\boldsymbol{r})$ under the WS-cell charge-neutrality constraint, $\int\mathrm{d}^3\boldsymbol{r}\,\rho(\boldsymbol{r})=0$—see the derivation making use of a Lagrange multiplier in Appendix A—yields the equilibrium counterion profile in terms of the Boltzmann factor

$$\overline{n}_+(\boldsymbol{r})=\frac{Z\mathrm{e}^{-\overline{\psi}(\boldsymbol{r})}}{\int\mathrm{d}^3\boldsymbol{r}\,\mathrm{e}^{-\overline{\psi}(\boldsymbol{r})}}=\frac{n_\mathrm{c}\exp[\langle\overline{\psi}\rangle-\overline{\psi}(\boldsymbol{r})]}{\langle\exp[\langle\overline{\psi}\rangle-\overline{\psi}(\boldsymbol{r})]\rangle}, \qquad n_\mathrm{c}\equiv\langle\overline{n}_+(\boldsymbol{r})\rangle=\frac{Z}{V}, \tag{3}$$

where we introduced the *effective* average density $n_\mathrm{c}$ of counterions in the free volume $V$ unoccupied by the polyion core, and the brackets denote unweighted spatial averages over $V$, $\langle\mathcal{X}(\boldsymbol{r})\rangle\equiv\int\mathrm{d}^3\boldsymbol{r}\,\mathcal{X}(\boldsymbol{r})/\int\mathrm{d}^3\boldsymbol{r}$. Substituting the equilibrium counterion profile $\overline{n}_+(\boldsymbol{r})$ into the Poisson equation leads to the PB equation, that needs to be solved numerically in the case of spherical polyions.

The Helmholtz free energy, $F\equiv\mathcal{F}[\overline{n}_+(\boldsymbol{r})]$, is obtained by evaluating the functional $\mathcal{F}$ at the optimized profile $n_+(\boldsymbol{r})=\overline{n}_+(\boldsymbol{r})$. It can be shown—cf. Sec. 3 of Ref. 18—that the nonlinear osmotic pressure $P\equiv-\mathrm{d}F/\mathrm{d}V$ (over pure solvent) is simply given by

$$\beta P=\overline{n}_+(R), \tag{4}$$

which is the well-know WS-cell mean-field result that the salt-free osmotic pressure is related to the counterion density at the WS-cell boundary[52,53] $r\equiv|\boldsymbol{r}|=R$. Henceforth, to simplify the notation, we will omit the bar to denote equilibrium properties.

## III. LINEARIZATION SCHEME

### A. In the presence of neutralizing counterions only

Let us introduce a linearized free-energy functional $\mathcal{F}_\mathrm{DH}$ that will lead to DH-type equations of state for the salt-free model system defined in the previous section. We start by

Downloaded 12 Jul 2004 to 194.95.63.241. Redistribution subject to AIP license or copyright, see http://jcp.aip.org/jcp/copyright.jsp

truncating the expansion of the nonlinear PB Helmholtz free-energy functional (1) to the quadratic order in the difference $n_+(\boldsymbol{r})-n_c$

$$\beta\mathcal{F}_{DH}[n_+(\boldsymbol{r})]\equiv\frac{1}{8\pi\ell_B}\int d^3\boldsymbol{r}[\nabla\psi(\boldsymbol{r})]^2+Z[\ln(n_c\zeta_+^3)-1]+n_c\ln(n_c\zeta_+^3)\int d^3\boldsymbol{r}\left[\frac{n_+(\boldsymbol{r})}{n_c}-1\right]+\frac{1}{2}n_c\int d^3\boldsymbol{r}\left[\frac{n_+(\boldsymbol{r})}{n_c}-1\right]^2. \quad (5)$$

Functional minimization of the linearized functional $\mathcal{F}_{DH}$ with respect to $n_+(\boldsymbol{r})$ under the WS-cell charge-neutrality constraint, $\int d^3\boldsymbol{r}\rho(\boldsymbol{r})=0$—performed in Appendix B with the use of a Lagrange multiplier—leads to the linearized equilibrium counterion profile and to the linearized DH-type equation for the electrostatic potential $\psi(\boldsymbol{r})$

$$n_+(\boldsymbol{r})=n_c[1+\langle\psi(\boldsymbol{r})\rangle-\psi(\boldsymbol{r})], \quad (6)$$

$$\nabla^2\psi(\boldsymbol{r})=\kappa^2[\psi(\boldsymbol{r})-\langle\psi(\boldsymbol{r})\rangle-1]+\frac{Z\ell_B}{a^2}\delta^3(|\boldsymbol{r}|-a), \quad (7)$$

with the inverse Debye screening length defined in terms of the averaged counterion density $n_c$

$$\kappa=\kappa_c\equiv\sqrt{4\pi\ell_B n_c}. \quad (8)$$

One should note that this is different from the standard linearized-PB treatment of the spherical WS cell—associated with the definition of a renormalized charge[54]—where the Debye screening length is defined in terms of the WS-cell boundary density $n_+(r=R)$. A detailed discussion comparing the two different linearization schemes—the standard one and the approach considered here—is performed in Appendix B, where the explicit solution to the electrostatic potential of the linearized DH-type Eq. (7) is also presented.

The linearized Helmholtz free energy, $F_{DH}\equiv\mathcal{F}_{DH}[n_+(\boldsymbol{r})]_{equil}$, is obtained by evaluating the linearized functional $\mathcal{F}_{DH}$, Eq. (5), at the optimized profile $n_+(\boldsymbol{r})$ satisfying Eqs. (6) and (7), and it is given explicitly by Eq. (B9) of Appendix B. The linearized osmotic pressure (over pure solvent) of the colloidal suspension follows from the negative *total derivative* of the linearized Helmholtz free energy $F_{DH}$ with respect to the WS-cell free volume $V$, $P_{DH}\equiv-dF_{DH}/dV$,

$$\beta P_{DH}=n_c\left\{1+\frac{Z\kappa\ell_B}{4\Delta_2^2(\kappa R,\kappa a)}\left[\frac{\Delta_1(\kappa R,\kappa a)}{\kappa a}\times[\Delta_1(\kappa R,\kappa a)-\Delta_2(\kappa R,\kappa a)]-4\kappa a\left(1+\frac{2}{3}\kappa^2a^2-\kappa^2R^2\right)-\frac{4}{3}\kappa^3R^3\right]\right\}, \quad (9)$$

where we introduced the functions $\Delta_1(u,v)\equiv\Delta_+(u)e^v-\Delta_-(u)e^{-v}$, $\Delta_2(u,v)\equiv\Delta_+(u)\Delta_-(v)-\Delta_-(u)\Delta_+(v)$, and $\Delta_\pm(u)\equiv(1\pm u)e^{\mp u}$. To obtain Eq. (9) one should take into account both the explicit $R$ dependence as well as the volume dependence of the screening length $\kappa^{-1}$ when computing the total derivative, $d/dV=1/(4\pi R^2)\,\partial/\partial R-\kappa/(2V)\partial/\partial\kappa$. The first term of Eq. (9) represents the uniform counterion-density ideal-gas law, while the next term corresponds to the mean-field electrostatic corrections[55] due to *intracell* polyion–microion correlations. In Appendix C it is shown that the linearized osmotic pressure (9) can be also obtained by a *formal* differentiation of the linearized Helmholtz free energy $F_{DH}$ and that it also corresponds to a quadratic expansion of the nonlinear PB osmotic pressure (4). At the end of the next subsection we shall find that for sufficiently high surface charges or low temperatures the linearized osmotic pressure (9) is no longer a monotonic function of the WS-cell free volume $V$, which would imply a thermodynamical instability and an associated gas/liquid-like phase separation of the system—in contrast to the full nonlinear theory, which does not predict any instability.[56]

### B. In the presence of neutralizing counterions and added salt (canonical ensemble)

Let us now add a symmetric monovalent (1:1) salt to the system. We treat all microions at the same level of mean-field approximation, describing them by the average local number densities $n_\pm(\boldsymbol{r})$. We will not distinguish between counterions and positive ions derived from the salt dissociation. Therefore, $n_+(\boldsymbol{r})$ accounts both for counterions and positive salt ions (cations), while $n_-(\boldsymbol{r})$ represents the negative coions (anions). In terms of these number densities, the total charge number density and the total microionic density read, respectively,

$$\rho(\boldsymbol{r})=n_+(\boldsymbol{r})-n_-(\boldsymbol{r})-\frac{Z}{4\pi a^2}\delta^3(|\boldsymbol{r}|-a),$$

and

$$n(\boldsymbol{r})=n_+(\boldsymbol{r})+n_-(\boldsymbol{r}). \quad (10)$$

The effective average uniform densities of positive and negative microions are given by

$$c_\pm=\langle n_\pm(\boldsymbol{r})\rangle=\frac{Q_\pm}{V},\quad Q_+=Z+n_sV,\quad Q_-=n_sV, \quad (11)$$

where $n_s$ is the *a priori* known effective average salt concentration and $Q_\pm$ are the fixed total number of positive and negative microions inside a WS cell. Within the cell-model approximation the salt ions are evenly distributed between different cells and the average salt concentration $n_s$ is the same for each identical WS cell. We introduce the dimensionless parameter

$$s\equiv\frac{Q_-}{Z}=\frac{n_s}{n_c}, \quad (12)$$

which measures the contribution of the salt ions to the ionic strength in the suspension

$$I\equiv\tfrac{1}{2}(n_c+2n_s)=\tfrac{1}{2}(1+2s)n_c. \quad (13)$$

As in the previous subsection, we expand the nonlinear PB Helmholtz free-energy functional

Downloaded 12 Jul 2004 to 194.95.63.241. Redistribution subject to AIP license or copyright, see http://jcp.aip.org/jcp/copyright.jsp

$$\beta\mathcal{F}[n_\pm(\boldsymbol{r})]=\frac{1}{8\pi\ell_B}\int d^3\boldsymbol{r}[\nabla\psi(\boldsymbol{r})]^2+\sum_{i=\pm}\int d^3\boldsymbol{r}\,n_i(\boldsymbol{r}) \times\{\ln[n_i(\boldsymbol{r})\zeta_i^3]-1\}, \tag{14}$$

about the average uniform densities (11) up to quadratic order in the differences $n_\pm(\boldsymbol{r})-c_\pm$, to obtain the linearized Helmholtz free-energy functional

$$\begin{aligned}\beta\mathcal{F}_{\mathrm{DH}}[n_\pm(\boldsymbol{r})] &= \frac{1}{8\pi\ell_B}\int d^3\boldsymbol{r}[\nabla\psi(\boldsymbol{r})]^2+\sum_{i=\pm}Vc_i[\ln(c_i\zeta_i^3)-1] \\ &+\sum_{i=\pm}c_i\ln(c_i\zeta_i^3)\int d^3\boldsymbol{r}\left[\frac{n_i(\boldsymbol{r})}{c_i}-1\right] \\ &+\frac{1}{2}\sum_{i=\pm}c_i\int d^3\boldsymbol{r}\left[\frac{n_i(\boldsymbol{r})}{c_i}-1\right]^2,\end{aligned} \tag{15}$$

where $\zeta_\pm$ are the thermal de Broglie wavelengths of cations (including the positive counterions) and anions, respectively.

Functional minimization of the linearized functional $\mathcal{F}_{\mathrm{DH}}[n_\pm(\boldsymbol{r})]$ with respect to $n_\pm(\boldsymbol{r})$ under the WS-cell charge-neutrality constraint

$$\int d^3\boldsymbol{r}\,\rho(\boldsymbol{r})=0, \quad \text{or} \quad \int d^3\boldsymbol{r}\,[n_+(\boldsymbol{r})-n_-(\boldsymbol{r})]=Z, \tag{16}$$

—performed in Appendix D with the help of a Lagrange multiplier—leads to the linearized equilibrium density profiles and to the linearized DH-type equation for the electrostatic potential $\psi(\boldsymbol{r})$

$$n_\pm(\boldsymbol{r})=c_\pm[1\pm\langle\psi(\boldsymbol{r})\rangle\mp\psi(\boldsymbol{r})], \tag{17}$$

$$\nabla^2\psi(\boldsymbol{r})=\kappa^2\left[\psi(\boldsymbol{r})-\langle\psi(\boldsymbol{r})\rangle-\frac{1}{1+2s}\right]+\frac{Z\ell_B}{a^2}\delta^3(|\boldsymbol{r}|-a), \tag{18}$$

where the inverse of the Debye screening length is now given by

$$\kappa=\sqrt{8\pi\ell_B I}=\sqrt{4\pi\ell_B(1+2s)n_c}=\kappa_c\sqrt{1+2s}. \tag{19}$$

As discussed in Appendix D, the infinite-dilution limit ($R\to\infty$) of the linearized solution to the electrostatic potential $\psi(\boldsymbol{r})$ leads to the repulsive electrostatic component of the traditional DLVO[43,44] interaction potential.

The linearized Helmholtz free energy, $F_{\mathrm{DH}}\equiv\mathcal{F}_{\mathrm{DH}}[n_\pm(\boldsymbol{r})]_{\mathrm{equil}}$, is obtained by evaluating the linearized functional $\mathcal{F}_{\mathrm{DH}}[n_\pm(\boldsymbol{r})]$, Eq. (15), at the linearized optimized profiles $n_\pm(\boldsymbol{r})$ satisfying Eqs. (17) and (18), and it is given explicitly by Eq. (D8) in Appendix D. In this Appendix we also discuss the correspondence between the infinite-dilution limit ($R\to\infty$) of the excess Helmholtz free energy and the state-independent volume terms obtained by Roij *et al.*,[34] which have been claimed to drive a gas–liquid phase separation in dilute deionized aqueous colloidal suspensions. The linearized *canonical* osmotic pressure of the colloidal suspension follows from the negative *total derivative* of the linearized Helmholtz free energy $F_{\mathrm{DH}}$ with respect to the WS-cell free volume $V$, but keeping fixed the total amount of salt, $P_{\mathrm{DH}}^{\mathrm{can}}(\phi,s)\equiv-(dF_{\mathrm{DH}}/dV)_s$, where the subscript to the right of the total derivative emphasizes that the parameter $s$ remains fixed during the total differentiation with respect to $V$

$$\begin{aligned}\beta P_{\mathrm{DH}}^{\mathrm{can}}(\phi,s) &= (1+2s)n_c\left\{1+\frac{Z\kappa\ell_B}{4(1+2s)\Delta_2^2(\kappa R,\kappa a)}\left[\frac{\Delta_1(\kappa R,\kappa a)}{\kappa a}\right.\right. \\ &\times[\Delta_1(\kappa R,\kappa a)-\Delta_2(\kappa R,\kappa a)] \\ &\left.\left.-4\kappa a\left(1+\frac{2}{3}\kappa^2a^2-\kappa^2R^2\right)-\frac{4}{3}\kappa^3R^3\right]\right\},\end{aligned} \tag{20}$$

where $\kappa$ is a function of $(\phi,s)$ through Eq. (19), and the functions $\Delta_1,\Delta_2$ are defined after Eq. (9). In Appendix D it is shown that the linearized canonical osmotic pressure (20) corresponds to a quadratic truncation of the nonlinear PB canonical osmotic pressure (D2).

In the vanishing volume fraction of polyions (infinite-dilution) limit, $\phi=(a/R)^3\to0$, the linearized canonical osmotic pressure has the asymptotic behavior

$$\begin{aligned}\beta P_{\mathrm{DH}}^{\mathrm{can}} &= \frac{\theta(1+2s)\phi}{4\pi a^2\ell_B}\left[1-\frac{\theta}{10(1+2s)}\phi^{1/3}\right. \\ &\left.-\frac{4\theta^2}{175}\phi^{2/3}+\mathcal{O}(\phi)\right], \\ \theta &\equiv \frac{3Z\ell_B}{a}.\end{aligned} \tag{21}$$

This leads to the asymptotic linearized *canonical* inverse isothermal compressibility

$$\begin{aligned}\beta\chi_{\mathrm{can}}^{-1} &\equiv n_p\left(\frac{d\beta P_{\mathrm{DH}}^{\mathrm{can}}}{dn_p}\right)_s \\ &= Zn_p(1+2s)\left[1-\frac{2\theta}{15(1+2s)}\phi^{1/3}\right. \\ &\left.-\frac{4\theta^2}{105}\phi^{2/3}+\mathcal{O}(\phi)\right],\end{aligned} \tag{22}$$

where $n_p=(4\pi R^3/3)^{-1}$ is the polyion density of the suspension. In the presence of added salt, the stability of the suspension is associated to the positiveness of the eigenvalues of the associated Hessian matrix—as discussed in Appendix H—instead of simply being related to the positiveness of the canonical inverse isothermal compressibility $\chi_{\mathrm{can}}^{-1}$, as compared in Fig. 1. The infinite-dilution asymptotic behavior of the function $\Sigma(\phi,s)$, Eq. (H2)—whose vanishing defines the linearized canonical spinodal line—reads

$$\begin{aligned}\Sigma(\phi,s) &= \frac{\theta\phi}{1+s}\left[1-\frac{2\theta}{15}(1+2s)\phi^{1/3}\right. \\ &\left.-\frac{4\theta^2}{525}(5-4s-4s^2)\phi^{2/3}+\mathcal{O}(\phi)\right].\end{aligned} \tag{23}$$

In contrast to the semigrand-canonical case (to be treated in the next subsection), the suspension is thermodynamically stable in the infinite-dilution limit for any finite $s$ (canonical case), $\lim_{\phi\to0}\Sigma(\phi,s)>0$. However, as exemplified by the

Downloaded 12 Jul 2004 to 194.95.63.241. Redistribution subject to AIP license or copyright, see http://jcp.aip.org/jcp/copyright.jsp

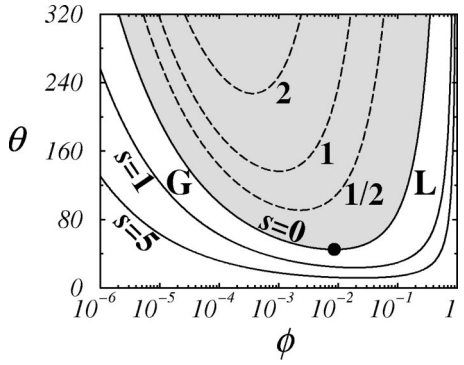


FIG. 1. Spinodal lines (solid lines) associated with the linearized *canonical* osmotic pressure $P_{\mathrm{DH}}^{\mathrm{can}}$, Eq. (20), in the $\theta=3Z\ell_B/a$ vs volume fraction $\phi=(a/R)^3$ plane. As explained in Appendix H, they correspond to lines of vanishing determinant of the associated Hessian matrix, and—except for the salt-free case—*do not coincide* with the lines of vanishing linearized canonical inverse isothermal compressibility, $\chi_{\mathrm{can}}^{-1}=0$ (dashed lines). In the gray region the linearized isothermal compressibility of the salt-free ($s=0$) suspension becomes negative, leading to a coexistence between gas (G) and liquid (L) fluid phases. The black circle represents the salt-free critical point (see main text for more details). Note that this is in contrast to the full nonlinear treatment, which *always* predicts positive compressibilities (Ref. 56). Addition of monovalent salt *enhances the instability* by shifting the canonical spinodal lines to lower values of $\theta$ (higher temperatures or lower polyion valences), as labeled by the two solid lines with increasing values of $s$. This is in contrast to a naive analysis based only on the vanishing of the canonical isothermal compressibility (dashed lines), which deceptively suggests exactly the opposite—namely, that addition of monovalent salt *would stabilize the suspension* against phase separation.

salt-free case in Fig. 2, for finite densities ($\phi\neq 0$) and sufficiently large values of $\theta$, the linearized canonical osmotic pressure $P_{\mathrm{DH}}^{\mathrm{can}}$ is no longer a convex function of the volume fraction $\phi$, implying thus the onset of a thermodynamical instability. For salt-free suspensions ($s=0$), the associated critical point—represented by the black circle in Fig. 1—is located at

$$\phi_{\mathrm{crit}}=0.008\,586\,189\cdots, \quad \theta_{\mathrm{crit}}=44.902\,477\,094\cdots, \tag{24}$$

which is determined by the criticality condition $\mathrm{d}P_{\mathrm{DH}}^{\mathrm{can}}/\mathrm{d}\phi=\mathrm{d}^2P_{\mathrm{DH}}^{\mathrm{can}}/\mathrm{d}\phi^2=0$. We should stress that the coexistence regions between the dilute gas (G) and the dense liquid (L) phases—limited by the binodal lines, not shown in Fig. 1—must be determined under the constraints of constant chemical potential of polyions $\mu_{\mathrm{p}}$ and of salt particles $\mu_{\mathrm{s}}$. Further details about how to determine the binodal lines are given in Appendix D. However, because the critical behavior is a spurious result of the linearization, it is not worthwhile to construct the phase diagrams in detail and we restrict ourselves only to present the spinodal lines in Fig. 1. Since the criticality condition defines where the binodal and the spinodal lines meet, the location of the critical points does not require computation of the binodal lines. In Appendix D we also discuss possible charge-renormalization[54,57,58] effects on the spurious phase separation predicted under linearization.

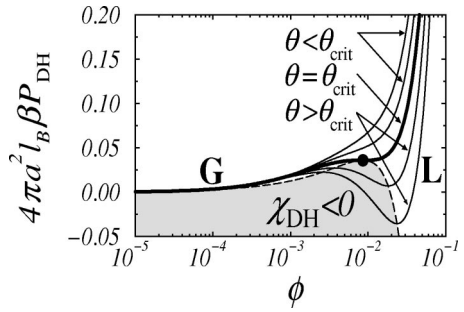


FIG. 2. Salt-free ($s=0$) linearized osmotic-pressure isotherms as a function of the volume fraction $\phi=(a/R)^3$. From top to bottom the isotherms correspond to $\theta=41,43,\theta_{\mathrm{crit}}=44.902\,477\cdots$(bold line), 47 and 49. In the gray region the salt-free linearized isothermal compressibility $\chi_{\mathrm{DH}}$ is negative, which would imply a thermodynamical instability that leads to a phase separation between two fluid phases: A low-$\phi$ (dilute) gas (G) and a high-$\phi$ (dense) liquid (L). The black circle represents the salt-free critical osmotic pressure and the dashed curve defines the salt-free spinodal line in the $\theta\times\phi$ diagram (the $s=0$ line in Fig. 1).

### C. In contact with an infinite salt reservoir (semigrand-canonical ensemble)

Let us now consider the colloidal suspension in electrochemical equilibrium with an infinite salt reservoir of fixed bulk density $n_{\mathrm{b}}$. The suspension is separated from the infinite reservoir by a semipermeable membrane. The solvent and microions (counterions and salt ions) can pass through the membrane, but not the large polyions. This gives rise to an imbalance in the osmotic pressure across the semipermeable membrane. This equilibrium between the suspension and the salt reservoir is referred to as a Donnan equilibrium.[9,59–61] Like in the previous subsections we will consider only the case of monovalent counterions and symmetric monovalent (1:1) salt.

The effective average salt concentration in the colloidal suspension, $n_{\mathrm{s}}\equiv\langle n_-(\boldsymbol{r})\rangle$, does not coincide with the reservoir bulk density $n_{\mathrm{b}}$ and is not known *a priori*. A nontrivial question is its dependence with the physical parameters of the system, e.g., bulk salt concentration $n_{\mathrm{b}}$, polyion radius $a$, polyion valence $Z$ and volume fraction $\phi\equiv(a/R)^3$. At the WS-cell PB mean-field level of approximation this problem has already been considered in the literature[62,63] and it is summarized in Appendix E. In agreement with exact and general results for WS-cell models,[56] the nonlinear osmotic pressure is a monotonic increasing function of the volume fraction $\phi$—hence the nonlinear treatment does not predict any thermodynamical instability.

Compared to the canonical case treated in the previous subsection—when the amount of microions is fixed and known *a priori*—there are two main differences to perform the linearization in the Donnan-equilibrium problem. First, because the Donnan equilibrium is established under constant electrochemical potential of microions, the natural thermodynamical ensemble to perform the calculations is the semigrand-canonical one

$$\Omega_{\mathrm{DH}}[n_\pm(\boldsymbol{r})]\equiv\mathcal{F}_{\mathrm{DH}}[n_\pm(\boldsymbol{r})]-\sum_{i=\pm}\mu_i\int \mathrm{d}^3\boldsymbol{r}\,n_i(\boldsymbol{r}),$$
$$\beta\mu_\pm=\ln(n_{\mathrm{b}}\zeta_\pm^3), \tag{25}$$

where we impose the equality of the microion electrochemical potentials inside the colloidal suspension, $\mu_\pm$, to the (mean-field) chemical potential of ideal gases of uniform density $n_{\mathrm{b}}$ for both types of ions in the infinite salt reservoir,

Downloaded 12 Jul 2004 to 194.95.63.241. Redistribution subject to AIP license or copyright, see http://jcp.aip.org/jcp/copyright.jsp

$\beta^{-1}\ln(n_b\zeta_\pm^3)$. The second difference is that the effective average uniform densities of positive and negative ions, about which the linearization should be performed, vary in a nontrivial way as the WS-cell free volume $V$ is changed. In Appendix F it is shown that the self-consistent linearized average densities for the Donnan problem are given by the state-independent zeroth-order Donnan densities

$$c_\pm^{(1)} \equiv \frac{\sqrt{n_c^2+(2n_b)^2}\pm n_c}{2}, \tag{26}$$

where $n_c = Z/V$ is the effective averaged counterion density and the superscript in $c_\pm^{(1)}$ emphasizes the fact that they were obtained under a linearized approximation. These correspond to the uniform densities that the system would have in the infinite-temperature ($\ell_B = 0$) limit under the constraint of overall WS-cell charge neutrality (16). We should remark that they *do not correspond* to the effective averages of the full nonlinear PB densities (E2)

$$c_\pm = \langle n_\pm(\boldsymbol{r})\rangle = \frac{\sqrt{n_c^2+(2n_b)^2\langle e^{\psi(\boldsymbol{r})}\rangle\langle e^{-\psi(\boldsymbol{r})}\rangle}\pm n_c}{2}, \tag{27}$$

because of the nonvanishing quadratic and higher-order ($\nu \geqslant 2$) contributions of the electrostatic potential differences

$$\delta_\nu(\boldsymbol{r}) \equiv [\langle\psi\rangle - \psi(\boldsymbol{r})]^\nu. \tag{28}$$

The nonlinear expression for $c_\pm$, Eq. (27), has been obtained by using an explicitly gauge-invariant formulation of the problem (cf. Appendix E). The advantage of these forms is that the linearized expansion densities (26) are simply obtained by taking their potential-independent, infinite-temperature ($\ell_B = 0$) limit, where the electrostatic-potential differences vanish, $\lim_{\ell_B\to 0}\delta_\nu(\boldsymbol{r})\to 0$. It is also clear that any other choice for the expansion densities will not lead to the exact potential-independent (infinite-temperature) limit of the nonlinear equations. As also derived in Appendix F, the Donnan average densities, Eqs. (26), do indeed correspond to the functional minimization of the corresponding linearized semigrand-canonical functional. We note that Deserno and von Grünberg[50] define an optimal linearization point $\bar{\psi}_{\rm opt}$—related to the above gauge-invariant expansion densities by $c_\pm^{(1)} = n_b e^{\mp\bar{\psi}_{\rm opt}}$—by using arguments based on the plausibility of this choice. They show that any other choice for the linearization point would lead to conflicting inequalities involving nonlinear and linearized averages. Finally, we should mention that even though the uniform expansion densities $c_\pm^{(1)}$, Eqs. (26), are *internally* self-consistent (within the semigrand-canonical ensemble) under linearization, *global* self-consistency (ensemble invariance) will require the use of the quadratic truncation of the nonlinear averages (27), $c_\pm = c_\pm^{(2)} + \mathcal{O}[\langle\delta_3(\boldsymbol{r})\rangle]$,

$$c_\pm^{(2)} \equiv \frac{\sqrt{n_c^2+(2n_b)^2 e^{\langle\delta_2(\boldsymbol{r})\rangle}}\pm n_c}{2}, \tag{29}$$

as the self-consistent averaged densities, as discussed in detail in Appendix G. Another way to look at this subtle point is by performing the Legendre transformation directly at level of the thermodynamic potential, $\Omega_{\rm DH} = F_{\rm DH} - \mu_+ Q_+ - \mu_- Q_-$—in contrast to perform it at the level of the functionals. An ensemble-invariant treatment of the Donnan effect—that relates the total charges inside the WS cell $Q_\pm = Vc_\pm \approx Vc_\pm^{(2)}$ with the average counterion density $n_c$ and the bulk salt concentration $n_b$—requires at the linearized level the use of $c_\pm^{(2)}$, Eqs. (29), as expansion densities—instead of the simplest $c_\pm^{(1)}$, Eqs. (26). The inclusion of the quadratic contributions into the expansion densities $c_\pm^{(2)}$, however, do not improve the agreement between the linearized and nonlinear equations, as can be shown by the explicit analytical comparison in the exactly solvable planar case.[51] However, this can only be verified *a posteriori*.

Once again, functional minimization of the linearized semigrand-canonical functional $\Omega_{\rm DH}[n_\pm(\boldsymbol{r})]$ with respect to $n_\pm(\boldsymbol{r})$ under the overall WS-cell charge-neutrality constraint (16)—performed in Appendix F with the help of a Lagrange multiplier—leads to the self-consistent linearized averaged densities (26), to the linearized equilibrium profiles and to the DH-type equation

$$n_\pm(\boldsymbol{r}) = c_\pm^{(1)}[1 \pm \langle\psi(\boldsymbol{r})\rangle \mp \psi(\boldsymbol{r})], \tag{30}$$

$$\nabla^2\psi(\boldsymbol{r}) = \kappa^2[\psi(\boldsymbol{r}) - \langle\psi(\boldsymbol{r})\rangle - \eta] + \frac{Z\ell_B}{a^2}\delta^3(|\boldsymbol{r}|-a), \tag{31}$$

where the parameter

$$\eta \equiv \frac{c_+^{(1)} - c_-^{(1)}}{c_+^{(1)} + c_-^{(1)}} = \frac{n_c}{\sqrt{n_c^2+(2n_b)^2}}, \tag{32}$$

measures the relative importance of the counterions to the ionic strength in the colloidal suspension

$$I \equiv \frac{1}{2}[c_+^{(1)} + c_-^{(1)}] = \frac{1}{2}\sqrt{n_c^2+(2n_b)^2} = \frac{n_c}{2\eta} = \frac{n_b}{\sqrt{1-\eta^2}}. \tag{33}$$

Furthermore, the (effective) Debye screening length $\kappa^{-1}$ in the colloidal suspension

$$\kappa^2 = 8\pi\ell_B I = \frac{\kappa_c^2}{\eta} = \frac{\kappa_b^2}{\sqrt{1-\eta^2}} > \kappa_b^2, \tag{34}$$

is always shorter than the Debye screening length $\kappa_b^{-1} \equiv 1/\sqrt{8\pi\ell_B n_b}$ associated with the bulk salt concentration $n_b$ in the reservoir, showing that screening is enhanced in the colloidal suspension compared to the salt reservoir.

The linearized semigrand-canonical potential, $\Omega_{\rm DH} \equiv \Omega_{\rm DH}[n_\pm(\boldsymbol{r})]_{\rm equil}$, is obtained by evaluating the linearized semigrand-canonical functional $\Omega_{\rm DH}[n_\pm(\boldsymbol{r})]$, Eq. (25), at the linearized optimized profiles $n_\pm(\boldsymbol{r})$ satisfying Eqs. (30) and (31), and it is given explicitly by Eq. (F11) of Appendix F. The linearized *semigrand-canonical* osmotic pressure follows from the negative *total derivative* of the linearized semigrand-canonical potential with respect to the WS-cell free volume $V$, but keeping fixed the microion chemical potentials $\mu_\pm$, $P_{\rm DH}^{\rm sgc}(\phi, n_b) \equiv -(d\Omega_{\rm DH}/dV)_{\mu_\pm}$

Downloaded 12 Jul 2004 to 194.95.63.241. Redistribution subject to AIP license or copyright, see http://jcp.aip.org/jcp/copyright.jsp

$$\beta P_{\mathrm{DH}}^{\mathrm{sgc}}(\phi,n_{\mathrm{b}})=\frac{n_{\mathrm{c}}}{\eta}\left\{1+\frac{\eta^2}{2}(\eta^2-1)+\frac{Z\kappa\ell_B\eta^3}{4\Delta_2^2(\kappa R,\kappa a)}\right.$$
$$\times\left[\frac{\Delta_1(\kappa R,\kappa a)}{\kappa a}[\Delta_1(\kappa R,\kappa a)-\Delta_2(\kappa R,\kappa a)]\right.$$
$$-4\kappa a\left(1+\frac{2\kappa^2a^2}{3\eta^2}-\kappa^2R^2\right)$$
$$\left.\left.-4\left(1-\frac{2}{3\eta^2}\right)\kappa^3R^3\right]\right\},\qquad(35)$$

where $\eta$ and $\kappa$ are functions of $(\phi,n_{\mathrm{b}})$ through Eqs. (32) and (34), respectively. The prefactor of the right-hand side represents the ideal-gas Donnan osmotic pressure taking only the WS-cell charge neutrality (16) into account

$$\frac{n_{\mathrm{c}}}{\eta}=c_+^{(1)}+c_-^{(1)}=\sqrt{n_{\mathrm{c}}^2+(2n_{\mathrm{b}})^2}.\qquad(36)$$

In analogy to the salt-free, Eq. (9), and the canonical, Eq. (20), cases, the first term of (35) represents the ideal-gas law associated to the state-independent zeroth-order Donnan densities, while the remaining terms correspond to the mean-field electrostatic corrections due to the microionic polarization around the polyion. We should note that the second term inside curly brackets depends on $\eta$ only and is thus $\ell_B$ independent. This could suggest that the zeroth-order Donnan ideal-gas law, $\lim_{\ell_B\to 0}\beta P_{\mathrm{DH}}^{\mathrm{sgc}}=n_{\mathrm{c}}/\eta$, would not be recovered in the weak-coupling limit. This $\ell_B$-independent term, however, is indeed necessary to cancel the contributions that arise from the last term in the $\ell_B\to 0$ limit in order to give the correct potential-independent infinite-temperature limit. Moreover, it is shown in Appendix E that the linearized semigrand-canonical osmotic pressure (35) corresponds to a quadratic expansion of the nonlinear semigrand-canonical osmotic pressure (E3). The ensemble equivalence between the linearized osmotic pressures $P_{\mathrm{DH}}^{\mathrm{can}}(\phi,s)$ and $P_{\mathrm{DH}}^{\mathrm{sgc}}(\phi,n_{\mathrm{b}})$, Eqs. (20) and (35), is nontrivial due to the Donnan effect. As discussed in detail in Appendix G, the linearized Legendre transformation $s=s(\phi,n_{\mathrm{b}})$ given by Eq. (G9) is not sufficient to ensure ensemble invariance, $P_{\mathrm{DH}}^{\mathrm{can}}[\phi,s(\phi,nb)]\neq P_{\mathrm{DH}}^{\mathrm{sgc}}(\phi,n_{\mathrm{b}})$, requiring additionally the inclusion of quadratic contributions in the expansion densities—i.e., $c_{\pm}^{(2)}$, Eqs. (29), should be used as expansion densities for the linearization, instead of $c_{\pm}^{(1)}$, Eqs. (26).

The linearized osmotic-pressure difference between the colloidal suspension and the infinite salt reservoir obeys $\beta\Delta P_{\mathrm{DH}}\equiv\beta P_{\mathrm{DH}}^{\mathrm{sgc}}-2n_{\mathrm{b}}=\beta P_{\mathrm{DH}}^{\mathrm{sgc}}-(n_{\mathrm{c}}/\eta)\sqrt{1-\eta^2}$, with $\beta P_{\mathrm{DH}}^{\mathrm{sgc}}$ given by Eq. (35). In Appendix I we show that the linearized semigrand-canonical osmotic-pressure difference $\beta\Delta P_{\mathrm{DH}}$ is intrinsically thermodynamically unstable in the infinite-dilution limit and we compare with expressions previously obtained by Deserno and von Grünberg.[50] In particular, the infinite-dilution ($\phi\to 0$) asymptotic linearized *semigrand-canonical* inverse isothermal compressibility

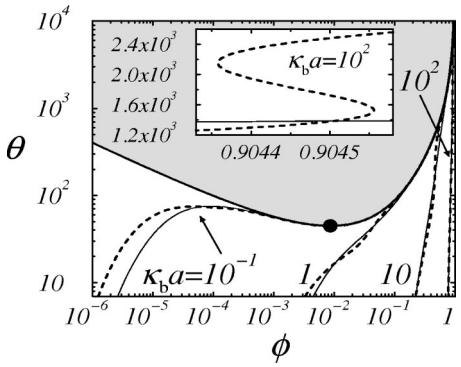


FIG. 3. Spinodal lines associated with the linearized *semigrand-canonical* osmotic pressure in the $\theta=3Z\ell_B/a$ vs volume fraction $\phi=(a/R)^3$ plane. Dashed lines, $\chi_{\mathrm{sgc}}^{-1}=0$, are associated to the internally self-consistent osmotic pressure $P_{\mathrm{DH}}^{\mathrm{sgc}}$, Eq. (35), while solid lines, $\hat{\chi}_{\mathrm{sgc}}^{-1}=0$, are associated to the globally self-consistent (ensemble-invariant) osmotic pressure $\hat{P}_{\mathrm{DH}}^{\mathrm{sgc}}$, Eq. (G13). The spinodal lines delimit the spurious unstable region that extends to lower values of $\phi$. To allow a comparison with the canonical case (Fig. 1), we also show the salt-free critical point (black circle) and the salt-free ($\kappa_{\mathrm{b}}a=0$) unstable gray region. In the salt-free limit ($\kappa_{\mathrm{b}}a\ll 1$) the semigrand-canonical spinodal line reduces to the salt-free one, although for any nonvanishing $\kappa_{\mathrm{b}}a$ eventually it will bend to the zero-temperature critical point at $(\phi_{\mathrm{crit}},\theta_{\mathrm{crit}})=(0,0)$. In agreement to the canonical case, an increase of the salt-reservoir bulk density $n_{\mathrm{b}}$ in the semigrand-canonical case also *enhances the instability*, as can be seen from the different spinodal lines with increasing $\kappa_{\mathrm{b}}a$. A typical nonmonotonic (but nonoscillating) osmotic-pressure isotherm is presented in Fig. 3 (dotted curve) of Ref. 50. See also Appendix I for additional comments.

$$\beta\chi_{\mathrm{sgc}}^{-1}\equiv n_{\mathrm{p}}\left(\frac{\mathrm{d}\beta P_{\mathrm{DH}}^{\mathrm{sgc}}}{\mathrm{d}n_{\mathrm{p}}}\right)_{\mu_\pm}$$
$$=-Zn_{\mathrm{p}}\theta^3\left\{\frac{\phi^2}{4\hat{a}^3(1+\hat{a})^2}+\frac{5\phi^3}{2\hat{a}^6}\left[\frac{2\hat{a}^3}{5(1+\hat{a})^2}-1\right]\right\}$$
$$+\mathcal{O}[\phi^4,\theta\phi^{-2/3}\exp(-2\hat{a}\phi^{-1/3})],\qquad(37)$$

—written in terms of the dimensionless variables $\theta\equiv 3Z\ell_B/a$ and $\hat{a}\equiv\kappa_{\mathrm{b}}a$—*is always negative*, in contrast to its canonical counterpart $\beta\chi_{\mathrm{can}}^{-1}$, Eq. (22), obtained at fixed ratio $s$.

In Fig. 3 we present the linearized semigrand-canonical spinodal lines, defined by the vanishing of the linearized *semigrand-canonical* inverse isothermal compressibility, $\chi_{\mathrm{sgc}}^{-1}=0$. We note that Figs. 1 and 3 cannot be, strictly speaking, interpreted as phase diagrams. Instead, their spurious spinodal lines should be viewed as an indication of the range of applicability of the linearized theory, which is asymptotically exact (at the PB-WS-model level) in the high-temperature limit. Furthermore, they illustrate that similar predictions of gas/liquid-like phase separation at low temperatures or high surface charges—which have also been predicted by other linearized theories, Refs. 33–40—are obtained for a thermodynamically self-consistent linearized theory.

## IV. CONCLUDING REMARKS

We investigated in detail the linearized PB spherical WS-cell model, by performing a linearization scheme consistent with quadratic expansions of the appropriate nonlin-

Downloaded 12 Jul 2004 to 194.95.63.241. Redistribution subject to AIP license or copyright, see http://jcp.aip.org/jcp/copyright.jsp

ear thermodynamic functional. By using gauge-invariant forms of the electrostatic potential, we have shown that the linearized osmotic pressures correspond to quadratic expansions of the corresponding nonlinear versions for the three cases investigated: In the presence of neutralizing counterions only (salt-free case), in the presence of fixed amount of added salt (canonical case) and in electrochemical equilibrium with an infinite salt-reservoir (Donnan equilibrium, semigrand-canonical case).

Contrary to previous works,[49,50] we adopted an explicitly gauge-invariant formulation with the inclusion of a Lagrange-multiplier term to account for the charge-neutrality constraint. The associated Lagrange multiplier was introduced in Appendices A–F in order to obtain the equilibrium profiles by functional minimization of the corresponding functional. In the case of the Donnan equilibrium, it is shown that the minimization of the associated linearized semigrand-canonical functional leads indeed to the state-independent zeroth-order Donnan densities as the self-consistent expansion averages for the linearization. Therefore the optimality of the optimal expansion point $\overline{\psi}_{\mathrm{opt}}$ introduced by Deserno and von Grünberg[50] can be understood as corresponding to a self-consistent minimization of the linearized functional. We would like to emphasize that the derivation of the expansion densities for the linearization, performed in Appendix F, does not correspond simply to an alternative way of obtaining the results presented in previous works.[49,50] In particular, we show in Appendix G that ensemble invariance of the linearized semigrand-canonical equations requires the inclusion of quadratic contributions in the expansion densities and in the linearized Legendre transformation, a point that could not be explored in Refs. 49 and 50.

It is shown that the self-consistent linearized osmotic pressure in the semigrand-canonical ensemble—as already pointed out in the literature[49,50]—leads to artifacts in the infinite-dilution, high-surface charge and strong-coupling limits, where it predicts negative isothermal compressibilities and negative osmotic-pressure differences between the colloidal suspension and the infinite salt reservoir. Attempts to define a fully stable linearized equation of state (for symmetric electrolytes) based on the partial derivative of the linearized semigrand-canonical potential with respect to the volume[50] cannot be justified in our approach based on the minimization of the linearized functional, its stability being a fortuitous result. This can be seen most clearly in the analytically tractable case of two infinite charged planes in electrochemical equilibrium with an infinite salt reservoir.[51] It turns out that the artifacts obtained by the linearization are not related to questions like thermodynamic self-consistency, ensemble invariance or possible alternative linearized osmotic-pressure definitions, but rather are associated to the application of the linearization outside its range of validity. Whereas in our treatment we are able to clearly identify the origin of the thermodynamical instability, the approximations involved in the linearized theories of Refs. 33–40 are far from being under control. Because the possible reasons for their failure are indeed very subtle, we believe our investigation about the linearization procedure in the well-controlled case of the PB WS-cell model sheds some light on this question, this being thus the main motivation of our study.

The linearization scheme presented here, though being fully thermodynamically self-consistent, shows that expressions obtained within a linearized framework should always be interpreted with caution, since they may lead to artifacts when applied outside their range of validity. As a further example where the linearization clearly yields artifacts, we mention the attractive component to the effective interaction between two confined colloids induced by charged walls, predicted under linearized theory[64] but in violation to the exact (at mean-field level) nonlinear PB repulsion.[65] Although earlier numerical analysis of the nonlinear solution were in agreement with the linearized theory,[66] these were soon ruled out under very general conditions.[65] The disagreement with the rigorous nonlinear results might be attributed to flaws in the numerical calculations. Attempts to include ionic correlations lead indeed to attractive contributions to the effective interaction,[67,68] but they are doubly-screened and thus are not able to overcome the repulsive electrostatic DLVO[43,44] component. Therefore, experimental evidences of confinement-induced attraction[69–71] and the occurrence of metastable superheated crystals[72] cannot be explained at the PB mean-field level and still remain an open question.[73] It is noteworthy that an explanation for the apparent attraction between like-charged colloids near *a single wall* has been recently proposed by Squires and Brenner,[74] where the attraction arises from nonequilibrium hydrodynamic flows. The estimated magnitude of this effect, however, seems to be too small to account for the attraction observed in the experiments,[75] besides the geometric constraint that the particles are in fact confined between *two walls*.

To avoid confusion we should stress at this point the exactness of the PB nonlinear solution at the mean-field level, its range of validity and limitations. In this work we discussed the linearization procedure in the framework of the nonlinear PB and the WS-cell model. The linearization constitutes here an approximation to the nonlinear treatment, whose exact results (at mean-field level) may be then compared to the linearized ones, allowing a control over the approximations and the onset of possible artifacts introduced by the linearization. The advantage of the treatment based on the linearization of the PB WS-cell model is that predictions of gas/liquid-like phase separation can be clearly traced back to artifacts due to the application of the linearization scheme beyond its range of validity. Of course, we are not able to predict correct results for real systems when the (starting) nonlinear theory itself breaks down. In this case, an eventual linearized result may *accidentally* lead to a correct prediction of, say, phase separation, due to the simultaneous application of two inadequate approximations, namely, the mean-field PB equation and its subsequent linearization. The fact that PB nonlinear theory for WS-cell models always leads to stable suspensions does not invalidate phase separation in real systems, which may be due to finite-size effects, *intra- and intercell* microion–microion, *intercell* polyion–polyion and *intercell* polyion–microion correlations that are neglected in the WS-cell mean-field PB picture. In the Donnan-equilibrium case, one should also take the microion–microion correlations in the infinite salt reservoir into

Downloaded 12 Jul 2004 to 194.95.63.241. Redistribution subject to AIP license or copyright, see http://jcp.aip.org/jcp/copyright.jsp

account. Questions related to this subject are far from being complete. In particular, it will be very interesting to look at the effect of charge renormalization[54,57,58] on the spurious predictions of the linearized theory and the inclusion of microionic–microionic correlations.[20]

Several linearized theories, Refs. 33–40, claim to theoretically explain the very puzzling physical phenomenon of gas/liquid-like phase separation in deionized aqueous suspensions of charged colloids mediated by monovalent counterions.[21–23] The phase transition predicted under linearized theories always points toward[33,34] the state-independent volume terms,[31,32] which are also responsible for the spurious phase separation observed by the linearization of the PB WS-cell model. We should remark that the negative contributions to the state-independent volume terms, Eq. (D11), originate from the polyion–counterion interaction free energy, its derivation being thus quite independent of the WS-cell model. Therefore, the identification that the state-independent volume terms drive the phase separation in linearized theories raises questions about the reliability of these results, since all linearized theories might suffer from exactly the same shortcomings. The predicted thermodynamical instability seems to be related to mathematical artifacts of the linearization itself and does not correspond thus to a real physical effect. The current theoretical description by linearized theories of the experimentally observed gas–liquid phase separation in deionized aqueous suspensions of charged colloids mediated by monovalent counterions[21–23] seems thus to be unsatisfactory. There is a need of more faithful theories or models—that should include correlation effects beyond the mean-field level—to describe this puzzling behavior.

## ACKNOWLEDGMENTS

The authors are grateful to M. Deserno and Y. Levin for the critical reading of the manuscript, for thoughtful and intensive discussions, and in particular to the former for kindly sharing his results on the Donnan linearization prior to publication. Discussions with H. H. von Grünberg and E. Trizac are also acknowledged. We would also like to thank the financial support by the Max-Planck-Gesellschaft and the Alexander von Humboldt-Stiftung.

[1] R. J. Hunter, *Introduction to Modern Colloid Science* (Oxford University Press, Oxford, 1993).
[2] D. F. Evans and H. Wennerström, *The Colloidal Domain: Where Physics, Chemistry, Biology, and Technology Meet*, 2nd ed. (Wiley, New York, 1999).
[3] H. Lodish, A. Berk, S. L. Zipursky, P. Matsudaira, D. Baltimore, and J. Darnell, *Molecular Cell Biology*, 4th ed. (W. H. Freeman, New York, 2000).
[4] B. Alberts, A. Johnson, J. Lewis, M. Raff, K. Roberts, and P. Walter, *Molecular Biology of the Cell*, 4th ed. (Garland, New York, 2002).
[5] C. Holm and K. Kremer, *Polyelectrolytes in Solution—Recent Computer Simulations*, in *Proceedings of the Yamada Conference on Polyelectrolytes*, edited by I. Noda and E. Kokufuta (Yamada Science Foundation, Osaka, 1999), p.27.
[6] C. Holm and K. Kremer, *Computer Simulations of Charged Systems*, in *Proceedings of the NATO Advanced Study Institute on Electrostatic Effects in Soft Matter and Biophysics*, edited by C. Holm, P. Kékicheff, and R. Podgornik (Kluwer, Dordrecht, 2001), p.117.
[7] H. L. Friedman and W. D. T. Dale, *Electrolyte Solutions at Equilibrium*, in *Statistical Mechanics, Part A: Equilibrium Techniques*, edited by B. J. Berne (Plenum, New York, 1977), Chap. 3, p.85.
[8] P. W. Debye and E. Hückel, Phys. Z. **24**, 185 (1923).
[9] T. L. Hill, *An Introduction to Statistical Thermodynamics* (Dover, New York, 1986).
[10] D. A. McQuarrie, *Statistical Mechanics* (Harper-Collins, New York, 1976).
[11] M. E. Fisher and Y. Levin, Phys. Rev. Lett. **71**, 3826 (1993); Y. Levin and M. E. Fisher, Physica A **225**, 164 (1996).
[12] K. S. Schmitz, *Macroions in Solution and Colloidal Suspension* (VCH, New York, 1993).
[13] Y. Levin, M. C. Barbosa, and M. N. Tamashiro, Europhys. Lett. **41**, 123 (1998).
[14] M. N. Tamashiro, Y. Levin, and M. C. Barbosa, Physica A **258**, 341 (1998).
[15] J. N. Israelachvili, *Intermolecular and Surface Forces*, 2nd ed. (Academic, London, 1992).
[16] S. A. Safran, *Statistical Thermodynamics of Surfaces, Interfaces and Membranes* (Addison-Wesley, Reading Mass., 1994).
[17] R. R. Netz and H. Orland, Eur. Phys. J. E **1**, 203 (2000).
[18] M. Deserno and C. Holm, *Cell Model and Poisson–Boltzmann Theory: A Brief Introduction*, in Ref. 6, p.27.
[19] See EPAPS Document No. E-JCPSA6-119-516326 for a mean-field approach to the Poisson–Boltzmann approximation. A direct link to this document may be found in the online article's HTML reference section. The document may also be reached via the EPAPS homepage (http://www.aip.org/pubservs/epaps.html) or from ftp.aip.org in the directory /epaps/. See the EPAPS homepage for more information.
[20] Y. Levin, Rep. Prog. Phys. **65**, 1577 (2002).
[21] N. Ise, T. Okubo, M. Sugimura, K. Ito, and H. J. Nolte, J. Chem. Phys. **78**, 536 (1983); S. Dosho, N. Ise, and K. Ito, *et al.* Langmuir **9**, 394 (1993); N. Ise, T. Konishi, and B. V. R. Tata, *ibid.* **15**, 4176 (1999).
[22] K. Ito, H. Hiroshi, and N. Ise, Science **263**, 66 (1994); B. V. R. Tata, E. Yamahara, P. V. Rajamani, and N. Ise, Phys. Rev. Lett. **78**, 2660 (1997).
[23] B. V. R. Tata, M. Rajalakshmi, and A. K. Arora, Phys. Rev. Lett. **69**, 3778 (1992).
[24] T. Palberg and M. Würth, Phys. Rev. Lett. **72**, 786 (1994).
[25] N. Grønbech-Jensen, K. M. Beardmore, and P. Pincus, Physica A **261**, 74 (1998).
[26] P. Linse and V. Lobaskin, Phys. Rev. Lett. **83**, 4208 (1999).
[27] E. Allahyarov and H. Löwen, Phys. Rev. E **63**, 041403 (2001).
[28] R. Messina, C. Holm, and K. Kremer, Phys. Rev. Lett. **85**, 872 (2000); Phys. Rev. E **64**, 021405 (2001).
[29] I. Sogami and N. Ise, J. Chem. Phys. **81**, 6320 (1984); M. V. Smalley, Mol. Phys. **71**, 1251 (1990); I. S. Sogami, T. Shinohara, and M. V. Smalley, *ibid.* **76**, 1 (1992); M. V. Smalley and I. S. Sogami, *ibid.* **85**, 869 (1995).
[30] L. Belloni, J. Phys.: Condens. Matter **12**, R549 (2000).
[31] B. Beresford-Smith, D. Y. C. Chan, and D. J. Mitchell, J. Colloid Interface Sci. **105**, 216 (1985).
[32] D. Y. C. Chan, Phys. Rev. E **63**, 061806 (2001).
[33] R. van Roij and J.-P. Hansen, Phys. Rev. Lett. **79**, 3082 (1997).
[34] R. van Roij, M. Dijkstra, and J.-P. Hansen, Phys. Rev. E **59**, 2010 (1999).
[35] J.-P. Hansen and H. Löwen, Annu. Rev. Phys. Chem. **51**, 209 (2000).
[36] P. B. Warren, J. Chem. Phys. **112**, 4683 (2000).
[37] A. R. Denton, Phys. Rev. E **62**, 3855 (2000).
[38] D. Y. C. Chan, P. Linse, and S. N. Petris, Langmuir **17**, 4202 (2001).
[39] S. N. Petris and D. Y. C. Chan, J. Chem. Phys. **116**, 8588 (2002).
[40] L. B. Bhuiyan and C. W. Outhwaite, J. Chem. Phys. **116**, 2650 (2002).
[41] J. Th. G. Overbeek, J. Chem. Phys. **87**, 4406 (1987); C. E. Woodward, *ibid.* **89**, 5140 (1988); J. Th. G. Overbeek, Mol. Phys. **80**, 685 (1993); Y. Rosenfeld, Phys. Rev. E **49**, 4425 (1994); D. G. Hall, Langmuir **12**, 4308 (1996); E. Trizac, *ibid.* **17**, 4793 (2001).
[42] K. S. Schmitz and L. B. Bhuiyan, Langmuir **18**, 1457 (2002); K. S. Schmitz, Phys. Rev. E **65**, 061402 (2002).
[43] B. V. Derjaguin and L. Landau, Acta Physicochim. URSS **14**, 633 (1941).
[44] E. J. W. Verwey and J. Th. G. Overbeek, *Theory of the Stability of Lyophobic Colloids* (Dover, New York, 1999).
[45] P. Linse and V. Lobaskin, J. Chem. Phys. **112**, 3917 (2000); P. Linse, *ibid.* **113**, 4359 (2000); V. Lobaskin, A. Lyubartsev, and P. Linse, Phys. Rev. E **63**, 020401 (2001).
[46] C. Holm and F. Mühlbacher (private communication).
[47] V. Lobaskin (private communication).
[48] A. Diehl, M. C. Barbosa, and Y. Levin, Europhys. Lett. **53**, 86 (2001).

Downloaded 12 Jul 2004 to 194.95.63.241. Redistribution subject to AIP license or copyright, see http://jcp.aip.org/jcp/copyright.jsp

[49] H. H. von Grünberg, R. van Roij, and G. Klein, Europhys. Lett. **55**, 580 (2001).
[50] M. Deserno and H. H. von Grünberg, Phys. Rev. E **66**, 011401 (2002).
[51] M. N. Tamashiro and H. Schiessel (unpublished).
[52] R. A. Marcus, J. Chem. Phys. **23**, 1057 (1955).
[53] H. Wennerström, B. Jönsson, and P. Linse, J. Chem. Phys. **76**, 4665 (1982).
[54] S. Alexander, P. M. Chaikin, P. Grant, G. J. Morales, P. Pincus, and D. Hone, J. Chem. Phys. **80**, 5776 (1984).
[55] We should stress that the electrostatic correction given by Eq. (9) was obtained by a linearization of the PB WS-cell functional, that takes only *intracell* polyion–microion correlations (at the mean-field level) into account. Therefore, it does not include any (neither inter- nor intracell) microion–microion correlations or *intercell* polyion–microion and polyion–polyion correlations. In the case of the (symmetric) RPM, where the mean-field contribution vanishes and only the microion–microion correlations are present, these lead to the famous Debye–Hückel electrostatic osmotic-pressure limiting law (Ref. 20), $-\kappa^3/(24\pi)$.
[56] G. Téllez and E. Trizac, J. Chem. Phys. **118**, 3362 (2003).
[57] L. Belloni, Colloids Surf. A **140**, 227 (1998).
[58] L. Bocquet, E. Trizac, and M. Aubouy, J. Chem. Phys. **117**, 8138 (2002); E. Trizac, L. Bocquet, and M. Aubouy, Phys. Rev. Lett. **89**, 248301 (2002); E. Trizac, M. Aubouy, and L. Bocquet, J. Phys.: Condens. Matter **15**, S291 (2003); E. Trizac, L. Bocquet, M. Aubouy, and H. H. von Grünberg, Langmuir **19**, 4027 (2003).
[59] F. G. Donnan, Chem. Rev. **1**, 73 (1924).
[60] J. Th. G. Overbeek, Prog. Biophys. Biophys. Chem. **6**, 57 (1956).
[61] T. L. Hill, Discuss. Faraday Soc. **21**, 31 (1956); J. Phys. Chem. **61**, 548 (1957).
[62] V. Reus, L. Belloni, T. Zemb, N. Lutterbach, and H. Versmold, J. Phys. II **7**, 603 (1997).
[63] M. N. Tamashiro, Y. Levin, and M. C. Barbosa, Eur. Phys. J. B **1**, 337 (1998).
[64] D. Goulding and J.-P. Hansen, Europhys. Lett. **46**, 407 (1999).
[65] J. C. Neu, Phys. Rev. Lett. **82**, 1072 (1999); J. E. Sader and D. Y. C. Chan, J. Colloid Interface Sci. **213**, 268 (1999); **218**, 423 (1999); Langmuir **16**, 324 (2000); E. Trizac, Phys. Rev. E **62**, R1465 (2000).
[66] W. R. Bowen and A. O. Sharif, Nature (London) **393**, 663 (1998); **402**, 841 (1999).
[67] O. Spalla and L. Belloni, Phys. Rev. Lett. **74**, 2515 (1995); L. Belloni and O. Spalla, J. Chem. Phys. **107**, 465 (1997).
[68] Y. Levin, Physica A **265**, 432 (1999).
[69] G. M. Kepler and S. Fraden, Phys. Rev. Lett. **73**, 356 (1994).
[70] M. D. Carbajal-Tinoco, F. Castro-Roman, and J. L. Arauz-Lara, Phys. Rev. E **53**, 3745 (1996).
[71] J. C. Crocker and D. G. Grier, Phys. Rev. Lett. **77**, 1897 (1996).
[72] A. E. Larsen and D. G. Grier, Phys. Rev. Lett. **76**, 3862 (1996); Nature (London) **385**, 230 (1997).
[73] D. G. Grier and J. C. Crocker, Phys. Rev. E **61**, 980 (2000).
[74] T. M. Squires and M. P. Brenner, Phys. Rev. Lett. **85**, 4976 (2000).
[75] Y. O. Popov, J. Colloid Interface Sci. **252**, 320 (2002).

**Downloaded 12 Jul 2004 to 194.95.63.241. Redistribution subject to AIP license or copyright, see http://jcp.aip.org/jcp/copyright.jsp**